

MHGNet: Multi-Heterogeneous Graph Neural Network for Traffic Prediction

Mei Wu

Hangzhou Dianzi University
Hangzhou, China
222320007@hdu.edu.cn

Yiqian Lin

Hangzhou Dianzi University
Hangzhou, China
linyq@hdu.edu.cn

Tianfan Jiang

Hangzhou Dianzi University
Hangzhou, China
232320005@hdu.edu.cn

Wenchao Weng*

Zhejiang University of Technology
Hangzhou, China
111124120010@zjut.edu.cn

Abstract—In recent years, traffic flow prediction has played a crucial role in the management of intelligent transportation systems. However, traditional forecasting methods often model non-Euclidean low-dimensional traffic data as a simple graph with single type nodes and edges, failing to capture similar trends among nodes of the same type. This paper proposes MHGNet, a new framework for modeling spatiotemporal multi-heterogeneous graphs, in which the STD Module decouples single-pattern traffic data into multi-pattern traffic data through feature mappings of timestamp embedding matrices and node embedding matrices. Then the Node Clusterer uses the Euclidean distance between nodes and different types of limit points for $O(N)$ time complexity clustering, and the nodes within clusters undergo residual subgraph convolution in the spatiotemporal fusion subgraphs generated by the DSTGG Module before entering the SIE Module for node repositioning and redistribution of weights. This paper conducts a series of ablation and quantitative evaluations on four widely used benchmarks to validate the effectiveness of MHGNet.

Index Terms—Traffic Prediction, Multi-Heterogeneous Graph, Traffic Patterns Decoupling, Subgraph Convolution

I. INTRODUCTION

The task of traffic prediction (e.g., traffic flow prediction) is based on historical traffic conditions collected from sensors to forecast future traffic conditions [1]–[3]. Graph Neural Networks (GNN) have been introduced to effectively manage the non-uniform topological structure of urban traffic networks [4]–[6]. Spatiotemporal Graph Neural Networks (STGNN) combine GNN with various temporal learning methods to capture hidden patterns of spatially irregular signals that change over time, thus addressing the spatiotemporal heterogeneity of non-Euclidean urban data [7]–[9]. However, existing models still cannot address the following issues in building spatiotemporal relationships between graph nodes:

(1) Lack of handling the structural patterns of traffic. Traffic signal features are contributed by multiple traffic patterns (e.g., trucks, passenger cars, broken-down vehicles). As shown in Figure 1, nodes with similar traffic patterns have similar flow (speed) changes, regardless of physical spatial distance.

(2) Lack of handling multi-dimensional spatiotemporal relationships. Current methods typically use Graph Neural Networks (GNN) to aggregate spatial features of single-dimensional flow or speed, and then use RNN or TCN for

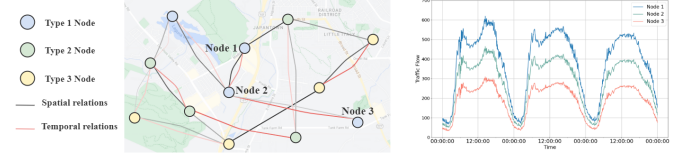


Fig. 1: The nodes have different sizes of spatiotemporal relationship similarities. Nodes of the same type have similar traffic patterns.

temporal feature extraction [10]–[12]. In reality, true traffic data is dynamically complex, exhibiting multi-dimensional spatiotemporal heterogeneity [13]–[15] within the spatial area of each node.

(3) Lack of diversity in modeling. Existing methods typically model non-Euclidean traffic data as simple graphs with single-type nodes and edges [16]–[18]. However, real-world complex traffic data, as shown in Figure 1, is a multigraph with various types of nodes and edges. The traffic flow of nodes of the same type shows similar trends, and node pairs are connected by two types of edges: temporal and spatial relationships.

To address issues one and two, the Spatiotemporal Decoupling Module in MHGNet is designed to decouple single-pattern traffic data into multi-pattern traffic data through the feature mapping of the timestamp embedding matrix and node embedding matrix, capturing dynamic multi-dimensional spatiotemporal information in the traffic pattern structure. For issue three, the complex traffic network is modeled as a multi-layer heterogeneous graph. A node clustering algorithm is employed, which clusters nodes by calculating the Euclidean distance between the nodes in a multi-dimensional feature space and different types of centroid points. The node sequence numbers are then stored in a node sequence pool.

As shown in Figure 2, the dynamic spatiotemporal graph generation module creates dynamic spatiotemporal subgraphs with weighted spatiotemporal relationships for each node cluster. This enables convolution operations on smaller, simpler homomorphic graphs rather than on large, complex heterogeneous graphs, effectively reducing time complexity and conserving computational resources. Finally, the clustered node IDs from the node sequence pool are used for

*corresponding author: 111124120010@zjut.edu.cn

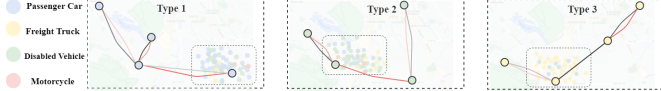


Fig. 2: Transforming multi-heterogeneous graph into simple subgraph convolution, with different types of nodes contributing traffic features from different traffic pattern structures.

regressing the node features after subgraph convolution. Two-dimensional convolution and a learnable parameter matrix adjust the weights of the subgraph convolution results at different scales, aggregating the output to iteratively update the sequence dependencies. In summary, the main contributions of this paper are as follows:

- This paper proposes a spatiotemporal modeling method for traffic prediction using heterogeneous multigraphs, mapping single-dimensional traffic data into a multi-dimensional feature space. A node clustering mechanism and a dynamic spatiotemporal graph generation module are employed to convert heterogeneous multigraphs into simple homomorphic graphs.
- A subgraph information extraction module is designed to perform gated spatiotemporal information extraction and weight adjustment of convolutional blocks at different scales, with the extracted information regressed back to the original positions of the clustered nodes.
- Comprehensive experiments were conducted on two well-known traffic flow datasets and two traffic speed datasets, demonstrating that MHNNet consistently outperforms various competitive baselines.

II. METHODOLOGY

In this section, we will elaborate on the proposed framework and its components. An overview of our model architecture is illustrated in Figure 3.

A. STD Module

To obtain heterogeneous spatiotemporal feature mappings for different traffic patterns, we introduce daily and weekly periodic feature matrices $T^D \in \mathbb{R}^{T_h \times N \times D_t}$ and $T^W \in \mathbb{R}^{T_h \times N \times D_t}$ into the STD Module, and then utilize a node embedding matrix $E \in \mathbb{R}^{N \times D_s}$ to weight and partition the original traffic flow $X_{t-T_h:t}$ into P types of traffic pattern features.

$$\begin{aligned} \Omega_{(t,i)} &= \text{Sigmoid}((\text{ReLU}(T_{(t,i)}^D || T_{(t,i)}^W || E_i)W_1)W_2) \\ X_n &= \hat{X}_{t-T_h:t} \odot \Omega_n \\ X_p &= \hat{X}_{t-T_h:t} - \sum_{n=1}^{p-1} X_n \end{aligned} \quad (1)$$

Here $\Omega_{(t,i)}$ represents the output proportion of the specific traffic pattern at node i relative to total traffic at time step t .

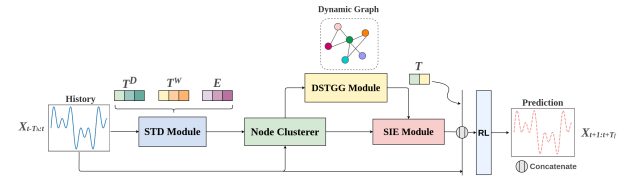


Fig. 3: Overall framework diagram (MHNNet)

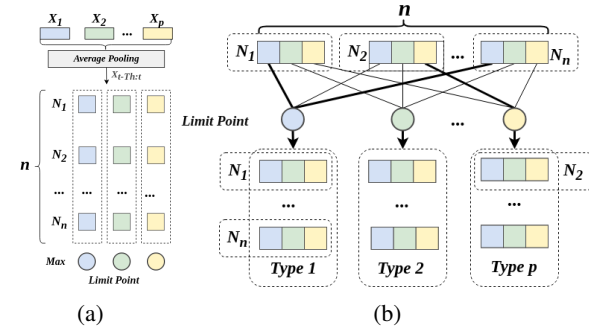


Fig. 4: (a) Constructing the limit point. (b) Clustering the nodes using the Euclidean distance.

B. Node Clusterer

As illustrated in Figure 4a, the clustering feature space is constructed based on the P types of traffic patterns:

$$\begin{aligned} R_t &= \frac{(X_1 W_1 || X_2 W_2 \dots || X_P W_P)}{\hat{X}_{t-T_h:t} W} \\ R &= \frac{1}{T_h} \sum_{t=1}^{T_h} R_t \\ C_j &= \text{Max}(R_j), \quad j = 1, 2, \dots, P \end{aligned} \quad (2)$$

The weight matrices $W_i \in \mathbb{R}^{D \times 1}$ for $i = 1, 2, \dots, P$ transform the enriched multi-dimensional features into a single dimension. We determine the maximum value of R across the P dimensions, resulting in the limit point matrix $C \in \mathbb{R}^P$, where C_p represents the maximum extremum state of the original traffic feature associated with feature P .

$$\begin{aligned} D_{i,j} &= |R_{i,j} - C_j|, \quad j = 1, 2, \dots, P \\ T_i &= \text{argmin}(D_{i,j}), \quad i \in S_T \end{aligned} \quad (3)$$

As shown in Figure 4b, the Euclidean distance matrix $D \in \mathbb{R}^{N \times P}$ is calculated between the feature tensor R and the limit point matrix C in the P -dimensional space. The type $T_i \in \mathbb{R}^1$ of node i is the type of the limit point with the minimum Euclidean distance, placing i in the node sequence pool S_T for type T_i , which is used for subsequent node placement. The time complexity of this clustering algorithm is $O(N)$, which significantly saves computational resources compared to traditional clustering algorithms.

C. DSTGG Module

We introduce the STGG Module to model the pairwise latent spatiotemporal relationships between subsets of nodes,

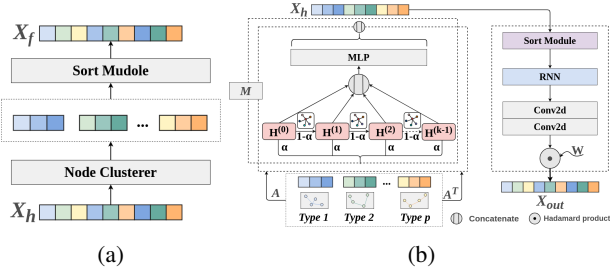


Fig. 5: (a) Node clustering and node repositioning demonstration. (b) SIE Module schematic diagram.

generating a simple subgraph containing spatiotemporal fusion relationships.

$$\begin{aligned} M_1 &= \tanh(\alpha E_p^1 W_1) \\ M_2 &= \tanh(\alpha E_p^2 W_2) \\ \hat{A}_p^s &= \alpha(M_1 M_2^T - M_1^T M_2) \end{aligned} \quad (4)$$

The matrices $E_p^1 \in \mathbb{R}^{N_p \times D_s}$ and $E_p^2 \in \mathbb{R}^{N_p \times D_s}$ represent the node embeddings for cluster P that are randomly initialized. The adjacency matrix $\hat{A}_p^s \in \mathbb{R}^{N_p \times N_p}$ containing the spatial relationships of cluster P is generated.

$$\begin{aligned} \hat{T}_p^D &= (T_i^D \parallel \dots \parallel T_{i+N_p}^D), \quad \{i, \dots, i+N_p\} \subseteq V_p \\ \hat{T}_p^W &= (T_i^W \parallel \dots \parallel T_{i+N_p}^W), \quad \{i, \dots, i+N_p\} \subseteq V_p \\ A_p^t &= \hat{T}_p^D \left(\hat{T}_p^W \right)^T \\ \hat{A}_p^t &= \beta \left(\text{ReLU} \left(\tanh \left(\frac{1}{T_h} \sum_{j=1}^{T_h} A_p^t[j, :] \right) \right) \right) \end{aligned} \quad (5)$$

The matrix $A_p^t \in \mathbb{R}^{T_h \times N_p \times N_p}$ captures the periodic temporal features of daily and weekly patterns. By applying average pooling and non-linear transformations, we obtain the fused temporal information matrix \hat{A}_p^t within the T_h time window for cluster P .

$$\begin{aligned} A_p &= \text{ReLU} \left(\tanh \left(\beta \hat{A}_p^s \left(\hat{A}_p^t \right)^T \right) \right) \\ \hat{A}_p &= \begin{cases} A_{i,j} & \text{if } j \in \text{argtopk}(A_p[i, :]) \\ 0 & \text{otherwise} \end{cases} \end{aligned} \quad (6)$$

Using the sparsified spatial graph and the fused temporal information matrix, we construct a simple graph containing heterogeneous spatiotemporal information.

D. SIE Module

This article introduces the SIE module, which is used to capture clustering features and spatiotemporal patterns in dynamic fused subgraphs, as shown in Figure 5.

To achieve information control and capture long-term dependencies, MHGNet introduces a gating mechanism in the graph convolution operation:

$$\tilde{A}_p = \hat{A}_p + I$$

$$\begin{aligned} H_p^{(k)} &= \gamma H_p + (1 - \gamma)(\tilde{D}^{-1} \tilde{A}) H_p^{(k-1)} \\ \hat{H}_p &= \left(H_p^{(0)} \parallel H_p^{(1)} \parallel \dots \parallel H_p^{(k-1)} \right) W \end{aligned} \quad (7)$$

In the formulas, let \tilde{A}_p denote the adjacency matrix that includes self-loops. The degree matrix $\tilde{D} \in \mathbb{R}^{N \times 1}$ is defined such that $\tilde{D}_{ii} = \sum_j \tilde{A}_{ij}$ for each node i . Additionally, the parameter k represents the depth of propagation.

$$\begin{aligned} X_h &= \left(\hat{H}_1 \parallel \hat{H}_2 \parallel \dots \parallel \hat{H}_p \right) \\ \hat{X}_h[:, i, :] &= X_h[:, j, :], \quad i \in S_N, j \in S_T \end{aligned} \quad (8)$$

In these equations, X_h represents the shuffled subgraph convolution results, S_N denotes a continuous permutation from 0 to N , and S_T is the node sequence pool generated by the Node Clusterer. The Sort Module regresses the node sequence, which is then used by the RNN to capture long-term temporal dependencies.

The model stacks the input over T_c time steps in the GRU to form an output tensor $H_{\text{out}} \in \mathbb{R}^{T_c \times N \times (M \times D)}$, and then performs weight redistribution on H_{out} :

$$\begin{aligned} H_{\text{out}} &= \text{dropout} \left([H^{(0)} \ H^{(1)} \ H^{(2)} \ \dots \ H^{(T_c-1)}] \right) \\ \hat{H}_{\text{out}} &= (\text{ReLU}(H_{\text{out}} * W_1) * W_2) \\ X_{\text{out}} &= \hat{H}_{\text{out}} \odot W \end{aligned} \quad (9)$$

E. Output and prediction

For the multi-scale spatiotemporal information captured by the SIE Module, we establish skip connections to incorporate additional feature information:

$$H = \{X_{\text{out}} \parallel X_{t-T_h:t} \parallel X_1 \parallel \dots \parallel X_p \parallel T^D \parallel T^W\} \quad (10)$$

The obtained tensor H is fed into the regression layer for feature integration and nonlinear transformation to obtain the prediction state $X_{t:t+T_f}$:

$$X_{t:t+T_f} = [(\text{ReLU}(\text{ReLU}(H)W_1)W_2) * W]^T \quad (11)$$

III. EXPERIMENTS

A. Datasets

We used two traffic flow datasets from the California Department of Transportation (CalTrans) Performance Measurement System (PEMS): PEMS04 and PEMS08, along with two traffic speed datasets: METR-LA and PEMS-BAY. The raw data is aggregated at 5-minute time intervals and organized according to predefined spatial graphs constructed based on real road networks. For detailed information about the aforementioned datasets, see Table I.

TABLE I: Dataset Statistics

Dataset	#Nodes	#Edges	#Days	#Data
PEMS04	307	340	59	16992
PEMS08	170	295	62	17856
METR-LA	207	1722	119	34272
PEMS-BAY	325	2694	181	52116

B. Baseline Methods

Baseline Methods: GWNet [19], DCRNN [20], STGCNDE [21], GMAN [22], AGCRN [23], STNorm [24], ASTGNN [25], STID [26], DDGCRN [27], PDFormer [28]

C. Experiment Settings

The experiment was conducted on a system equipped with an NVIDIA GeForce RTX 4090 GPU. The METR-LA and PEMS-BAY datasets were divided into training, testing, and validation sets in a 7:2:1 ratio. For the PEMS04 and PEMS08 datasets, we used a 6:2:2 split. The model was trained using the Adam optimizer, with a weight decay (wdecay) of 1.0×10^{-5} and an epsilon (eps) value of 1.0×10^{-8} . Implement a warm-up strategy during the first 20 training cycles, followed by curriculum learning with a length of 3. The model parameters for the four datasets are detailed in Table II. The source code of MHGNet is available: <https://github.com/meiwu5/MHGNet.git>

TABLE II: Model Parameters for Datasets

Dataset	Batch size	D_s	D_t	P	lr
PEMS04	64	10	10	3	0.006
PEMS08	64	10	10	3	0.006
METR-LA	32	10	10	2	0.002
PEMS-BAY	32	10	10	2	0.002

D. Experiment Results

TABLE III: The Average Metrics on the Traffic Flow Dataset.

Models	PEMS04			PEMS08		
	MAE	RMSE	MAPE	MAE	RMSE	MAPE
GWNet	19.36	31.72	13.30%	15.06	24.86	9.51%
DCRNN	19.63	31.26	13.59%	15.22	24.17	10.21%
STGCNDE	19.21	31.09	12.76%	15.45	24.81	9.92%
GMAN	19.14	31.60	13.19%	15.31	24.92	10.13%
AGCRN	19.38	31.25	13.40%	15.32	24.41	10.03%
STNorm	18.96	30.98	12.69%	15.41	24.77	9.76%
ASTGNN	18.60	31.03	12.63%	14.97	24.71	9.49%
DDGCRN	18.45	30.51	12.19%	14.40	23.75	9.40%
STID	18.38	29.95	12.04%	14.21	23.28	9.27%
PDFormer	18.36	30.03	12.00%	13.58	23.41	9.05%
MHGNet	18.32	29.96	12.30%	13.69	23.22	9.03%

As shown in Tables III and IV, our method achieves better performance across most metrics on all four datasets. We can draw the following conclusions: Compared to GNN-based models (such as DDGCRN and AGCRN), MHGNet

TABLE IV: Performance Metrics on the Traffic Speed Dataset

Dataset	Models	Horizon 3			Horizon 6			Horizon 12		
		MAE	RMSE	MAPE	MAE	RMSE	MAPE	MAE	RMSE	MAPE
METR-LA	AGCRN	2.87	5.58	7.70%	3.23	6.58	9.00%	3.62	7.51	10.38%
	STNorm	2.81	5.57	7.40%	3.18	6.59	8.47%	3.57	7.51	10.24%
	STID	2.82	5.53	7.75%	3.19	6.57	9.39%	3.55	7.55	10.95%
	PDFormer	2.83	5.45	7.77%	3.20	6.46	9.19%	3.62	7.47	10.91%
	MHGNet	2.80	5.52	7.58%	3.18	6.62	9.26%	3.54	7.56	10.75%
PEMS-BAY	AGCRN	1.37	2.87	2.94%	1.69	3.85	3.87%	1.96	4.54	4.64%
	STNorm	1.33	2.82	2.76%	1.65	3.77	3.66%	1.92	4.45	4.46%
	STID	1.31	2.79	2.78%	1.64	3.73	3.73%	1.91	4.42	4.55%
	PDFormer	1.32	2.83	2.78%	1.64	3.79	3.71%	1.91	4.43	4.51%
	MHGNet	1.31	2.74	2.75%	1.62	3.65	3.62%	1.90	4.36	4.43%

improves performance through subgraph-based heterogeneous graph modeling. Compared to embedding-based models like STID, it demonstrates better adaptability in handling complex traffic data. Additionally, when compared to attention-based models (such as ASTGNN and PDFormer), it exhibits good robustness and generalization performance, particularly excelling in the traffic speed dataset (such as PEMS-BAY).

TABLE V: Comparison of parameter count

Dataset	DDGCRN	STID	PDFormer	MHGNet ^φ	MHGNet
PEMS04	569254	121068	531165	655268	266470
PEMS08	311759	116684	531165	303139	166332

- **MHGNet^φ**: The variant with two layers of whole-graph convolution after removing the node classifier.

E. Ablation Experiments

TABLE VI: Node Clusterer Ablation

Dataset	Variants	Horizon 3			Horizon 6			Horizon 12		
		MAE	RMSE	MAPE	MAE	RMSE	MAPE	MAE	RMSE	MAPE
PEMS04	w/o Node Clusterer	17.81	28.89	11.86%	18.70	30.36	12.37%	20.30	32.61	13.42%
	MHGNet _{p=2}	17.57	28.76	11.69%	18.43	30.17	12.15%	19.78	32.18	13.18%
	MHGNet _{p=3}	17.48	28.63	11.73%	18.30	30.03	12.06%	19.69	32.07	12.96%
PEMS08	w/o Node Clusterer	13.81	22.08	9.00%	14.61	23.82	9.53%	16.09	26.38	10.57%
	MHGNet _{p=2}	12.84	21.54	8.41%	13.69	23.35	8.99%	15.76	26.06	10.29%
	MHGNet _{p=3}	12.77	21.54	8.47%	13.61	23.36	9.03%	15.58	25.93	10.20%
METR-LA	w/o Node Clusterer	2.83	5.53	7.67%	3.22	6.61	9.46%	3.76	7.77	11.67%
	MHGNet _{p=2}	2.80	5.52	7.58%	3.18	6.62	9.26%	3.54	7.56	10.75%
	MHGNet _{p=3}	2.80	5.56	7.59%	3.17	6.58	9.29%	3.56	7.58	10.98%
PEMS-BAY	w/o Node Clusterer	1.34	2.82	2.87%	1.66	3.77	3.74%	1.97	4.43	4.65%
	MHGNet _{p=2}	1.31	2.74	2.75%	1.62	3.65	3.62%	1.90	4.36	4.43%
	MHGNet _{p=3}	1.32	2.79	2.81%	1.63	3.72	3.70%	1.92	4.42	4.53%

- **w/o Node Clusterer**: No node clustering, perform a single graph convolution
- **MHGNet_{p=2}**: Node clustering into 2 patterns followed by subgraph convolution
- **MHGNet_{p=3}**: Node clustering into 3 patterns followed by subgraph convolution

TABLE VII: Spatiotemporal Graph Ablation.

Models	PEMS04			PEMS08		
	MAE	RMSE	MAPE	MAE	RMSE	MAPE
w/o sg	18.73	30.31	12.67%	14.07	23.43	9.19%
w/o tg	18.56	30.09	12.97%	14.08	23.50	9.29%
MHGNet _{p=2}	18.41	30.08	12.20%	13.81	23.31	9.08%

- **w/o sg**: Removing \hat{A}_p^s in the DSTGNN Module.
- **w/o tg**: Removing \hat{A}_p^t in the DSTGNN Module.
- **MHGNet_{p=2}**: Using the spatiotemporal fused graph \hat{A}_p .

IV. CONCLUSION

In this paper, we propose MHGNet, a new framework for modeling spatiotemporal heterogeneous graphs. The model utilizes a timestamp embedding matrix and a node embedding matrix to decouple one-dimensional features into a multi-dimensional feature space, enabling simple clustering. During the clustering process, a dynamic graph containing spatiotemporal information is generated for subgraph convolution. Moreover, experiments are conducted on multiple datasets.

REFERENCES

[1] D. A. Tedjopurnomo, Z. Bao, B. Zheng, F. M. Choudhury, and A. K. Qin, "A Survey on Modern Deep Neural Network for Traffic Prediction: Trends, Methods and Challenges," *IEEE Transactions on Knowledge and Data Engineering*, vol. 34, no. 4, pp. 1544–1561, 2022. [DOI: 10.1109/TKDE.2020.3001195].

[2] W. Shao *et al.*, "Long-term Spatio-Temporal Forecasting via Dynamic Multiple-Graph Attention," in *Proceedings of the Thirty-First International Joint Conference on Artificial Intelligence*, pp. 2225–2232, 2022. [DOI: 10.24963/ijcai.2022/309].

[3] Y. Lv, Y. Duan, W. Kang, Z. Li, and F.-Y. Wang, "Traffic Flow Prediction With Big Data: A Deep Learning Approach," *IEEE Transactions on Intelligent Transportation Systems*, vol. 16, no. 2, pp. 865–873, 2015. [DOI: 10.1109/TITS.2014.2345663].

[4] J. S. Gracias, G. S. Parnell, E. Specking, E. A. Pohl, and R. Buchanan, "Smart Cities—A Structured Literature Review," *Smart Cities*, vol. 6, no. 4, pp. 1719–1743, 2023. [DOI: 10.3390/smartcities6040080].

[5] Z. Liu, Z. Li, K. Wu, and M. Li, "Urban Traffic Prediction from Mobility Data Using Deep Learning," *IEEE Network*, vol. 32, no. 4, pp. 40–46, 2018. [DOI: 10.1109/MNET.2018.1700411].

[6] Z. Pan *et al.*, "Urban Traffic Prediction from Spatio-Temporal Data Using Deep Meta Learning," in *Proceedings of the 25th ACM SIGKDD International Conference on Knowledge Discovery & Data Mining*, pp. 1720–1730, 2019. [DOI: 10.1145/3292500.3330884].

[7] A. B. P and R. Sumathi, "Data Sources for Urban Traffic Prediction: A Review on Classification, Comparison and Technologies," in *2020 3rd International Conference on Intelligent Sustainable Systems (ICISS)*, pp. 628–635, 2020. [DOI: 10.1109/ICISS49785.2020.9316096].

[8] Z. Pan *et al.*, "Spatio-Temporal Meta Learning for Urban Traffic Prediction," *IEEE Transactions on Knowledge and Data Engineering*, vol. 34, no. 3, pp. 1462–1476, 2022. [DOI: 10.1109/TKDE.2020.2995855].

[9] F. Scarselli *et al.*, "The Graph Neural Network Model," *IEEE Transactions on Neural Networks*, vol. 20, no. 1, pp. 61–80, 2009. [DOI: 10.1109/TNN.2008.2005605].

[10] X. Wang *et al.*, "Traffic Flow Prediction via Spatial Temporal Graph Neural Network," in *Proceedings of The Web Conference 2020*, pp. 1082–1092, 2020. [DOI: 10.1145/3366423.3380186].

[11] H. Yao *et al.*, "Revisiting Spatial-Temporal Similarity: A Deep Learning Framework for Traffic Prediction," *Proceedings of the AAAI Conference on Artificial Intelligence*, vol. 33, no. 1, pp. 5668–5675, 2019. [DOI: 10.1609/aaai.v33i01.33015668].

[12] T. Liu *et al.*, "Graph-Based Dynamic Modeling and Traffic Prediction of Urban Road Network," *IEEE Sensors Journal*, vol. 21, no. 24, pp. 28118–28130, 2021. [DOI: 10.1109/JSEN.2021.3124818].

[13] Y. Shi *et al.*, "AspEm: Embedding Learning by Aspects in Heterogeneous Information Networks," 2018. [Online]. Available: <https://arxiv.org/abs/1803.01848>.

[14] Y. Shi *et al.*, "Easing Embedding Learning by Comprehensive Transcription of Heterogeneous Information Networks," in *Proceedings of the 24th ACM SIGKDD International Conference on Knowledge Discovery & Data Mining*, pp. 2190–2199, 2018. [DOI: 10.1145/3219819.3220006].

[15] S. Vashishth *et al.*, "Composition-based Multi-Relational Graph Convolutional Networks," 2020. [Online]. Available: <https://arxiv.org/abs/1911.03082>.

[16] X. Yin *et al.*, "Deep Learning on Traffic Prediction: Methods, Analysis, and Future Directions," *IEEE Transactions on Intelligent Transportation Systems*, vol. 23, no. 6, pp. 4927–4943, 2022. [DOI: 10.1109/TITS.2021.3054840].

[17] X. Shi *et al.*, "A Spatial-Temporal Attention Approach for Traffic Prediction," *IEEE Transactions on Intelligent Transportation Systems*, vol. 22, no. 8, pp. 4909–4918, 2021. [DOI: 10.1109/TITS.2020.2983651].

[18] M. Shaygan *et al.*, "Traffic prediction using artificial intelligence: Review of recent advances and emerging opportunities," *Transportation Research Part C: Emerging Technologies*, vol. 145, p. 103921, 2022. [DOI: 10.1016/j.trc.2022.103921].

[19] Z. Wu *et al.*, "Graph WaveNet for Deep Spatial-Temporal Graph Modeling," 2019. [Online]. Available: <https://arxiv.org/abs/1906.00121>.

[20] Y. Li, R. Yu, C. Shahabi, and Y. Liu, "Diffusion Convolutional Recurrent Neural Network: Data-Driven Traffic Forecasting," in *International Conference on Learning Representations*, 2018. [Online]. Available: <https://openreview.net/forum?id=SJiHXGWAZ>.

[21] J. Choi and N. Park, "Graph Neural Rough Differential Equations for Traffic Forecasting," *ACM Trans. Intell. Syst. Technol.*, vol. 14, no. 4, art. 74, 2023. [DOI: 10.1145/3604808].

[22] C. Zheng *et al.*, "GMAN: A Graph Multi-Attention Network for Traffic Prediction," 2019. [Online]. Available: <https://arxiv.org/abs/1911.08415>.

[23] L. Bai *et al.*, "Adaptive Graph Convolutional Recurrent Network for Traffic Forecasting," 2020. [Online]. Available: <https://arxiv.org/abs/2007.02842>.

[24] J. Deng *et al.*, "ST-Norm: Spatial and Temporal Normalization for Multi-variate Time Series Forecasting," in *Proceedings of the 27th ACM SIGKDD Conference on Knowledge Discovery & Data Mining*, pp. 269–278, 2021. [DOI: 10.1145/3447548.3467330].

[25] S. Guo *et al.*, "Learning Dynamics and Heterogeneity of Spatial-Temporal Graph Data for Traffic Forecasting," *IEEE Transactions on Knowledge and Data Engineering*, vol. 34, no. 11, pp. 5415–5428, 2022. [DOI: 10.1109/TKDE.2021.3056502].

[26] Z. Shao *et al.*, "Spatial-Temporal Identity: A Simple yet Effective Baseline for Multivariate Time Series Forecasting," in *Proceedings of the 31st ACM International Conference on Information & Knowledge Management*, pp. 4454–4458, 2022. [DOI: 10.1145/3511808.3557702].

[27] W. Weng *et al.*, "A Decomposition Dynamic Graph Convolutional Recurrent Network for Traffic Forecasting," *Pattern Recognition*, vol. 142, p. 109670, 2023. [DOI: 10.1016/j.patcog.2023.109670].

[28] J. Jiang *et al.*, "PDFormer: Propagation Delay-Aware Dynamic Long-Range Transformer for Traffic Flow Prediction," 2024. [Online]. Available: <https://arxiv.org/abs/2301.07945>.